

# GaInAsP/InP membrane lasers for optical interconnects

メタデータ	言語: eng 出版者: 公開日: 2017-10-03 キーワード (Ja): キーワード (En): 作成者: メールアドレス: 所属:
URL	<a href="http://hdl.handle.net/2297/29705">http://hdl.handle.net/2297/29705</a>

# GaInAsP/InP Membrane Lasers for Optical Interconnects

Shigehisa Arai, *Fellow, IEEE*, Nobuhiko Nishiyama, *Senior Member, IEEE*, Takeo Maruyama, *Member, IEEE*,  
and Tadashi Okumura, *Member, IEEE*

(Invited Paper)

**Abstract**—In this paper, the state-of-the art of long-wavelength GaInAsP/InP membrane semiconductor lasers, one of the most promising candidate light sources for optical interconnects and on-chip optical wiring between large-scale integrated circuits, is described. After an extensive review of research activities focused on laser preparation on either Si or Si-on-insulator substrate, the findings of our recent research activities on low power consumption lasers are presented. Specifically, our interest was set on the low-damage fabrication of strongly index-coupled grating, which is generally opted for DFB and distributed reflector (DR) lasers consisting of wire-like active regions, as well as of high index-contrast membrane waveguides. A submilliampere threshold current and a differential quantum efficiency close to 50% from the front facet were achieved in the case of the DR laser. On the other hand, a lateral current injection (LCI) structure, which can be combined with the membrane laser, was adopted for the realization of an injection-type membrane laser. The successful continuous wave operation of LCI lasers, prepared on a semiinsulating InP substrate, was achieved with moderately low threshold current at room temperature.

**Index Terms**—DFB laser, distributed reflector (DR) laser, GaInAsP/InP, optical interconnect, optical wiring, semiconductor laser, single-mode laser, Si-on-insulator (SOI) circuits, III–V materials.

## I. INTRODUCTION

SINCE the operating speed of large-scale integrated circuits (LSIs) is increasing year by year, following the miniaturization of process nodes,  $RC$  delay time and power dissipation of high-speed signal transmission between relatively distant points will eventually limit the performance of LSIs. Consequently, the

introduction of on-chip optical wiring has become one of the promising solutions to overcome this emerging problem [1]. Recently, enormous effort has been devoted to realize functional optical/photonic devices/integrated circuits on Si or Si-on-insulator (SOI) substrates by means of advanced Si-CMOS technologies [2]–[4], and a new field called “silicon photonics” is being established [5].

The optical absorption loss of single crystal Si becomes negligible at a wavelength longer than  $1.2\ \mu\text{m}$  even when it is used as a core material of optical waveguides such as a Si wire buried in  $\text{SiO}_2$  or a Si rib waveguide. The transmission loss of these waveguides is dominated by the scattering loss due to the interface roughness between high index contrast materials. In the past, an extremely low propagation loss of  $0.35\ \text{dB/cm}$ , which is, however, better than the value reported for optical waveguides consisting of III–V materials, has been demonstrated [6]. Passive optical components and functional photonic integrated circuits exhibiting extremely low scattering loss have also been reported, i.e., considerably low  $90^\circ$  bending loss of  $0.01\ \text{dB}$  with a  $2\ \mu\text{m}$  radius [7] and an extremely high  $Q$  factor exceeding 1000 000 with a 2-D photonic crystal (PC) resonator [8] were achieved using a SOI substrate with a Si layer of 200–300 nm thickness.

Since optical wiring is immune to the  $RC$  time delay and, furthermore, no skin effect is observed like in electrical wiring, it would be advantageous when the clock speed in the LSI becomes faster and faster. A multiple-core architecture with limited clock speed can open the way to the realization of LSIs based on existing mass-production technologies. Nonetheless, optical wiring would be only an alternative method in case the clock speed exceeds 10 GHz, because of the optical waveguide characteristics such as low loss and high speed as well as the low power consumption of existing high-speed photo detectors. Since the minimum receivable power of a typical PIN photodiode used for long wavelength optical fiber communications is  $-15\ \text{dB-m}$  (approximately  $30\ \mu\text{W}$ ) for 10 Gbit/s signals with a bit error rate (BER) of  $10^{-9}$ , the required output power of the light source will be of the order of hundreds of microwatt (for much lower BER); hence, the optical pulse energy is in the order of tens of femtojoule per bit. Such low power consumption has pushed rack-to-rack or board-to-board optical interconnections into modern supercomputers [9].

Recently, high-speed optical detectors as well as electro-optic modulators based on SOI substrates have been reported. Specifically, Ge detectors with such high speed as 30 GHz

Manuscript received December 19, 2010; revised February 25, 2011; accepted March 7, 2011. Date of publication April 21, 2011; date of current version October 5, 2011. This work was supported in part by the Ministry of Education, Culture, Sports, Science, and Technology (MEXT), Japan, under Grant-in-Aid for Scientific Research Nos. 19002009, 22360138, 21226010, 08J55211, and 10J08973, and in part by the Japan Society for the Promotion of Science (JSPS) under the JSPS-FIRST program.

S. Arai is with the Quantum Nanoelectronics Research Center, Tokyo Institute of Technology, Tokyo 152-8552, Japan (e-mail: arai@pe.titech.ac.jp).

N. Nishiyama and T. Okumura are with the Department of Electrical and Electronic Engineering, Tokyo Institute of Technology, Tokyo 152-8552, Japan (e-mail: n-nishi@pe.titech.ac.jp; tokumura@quantum.pe.titech.ac.jp).

T. Maruyama is with the School of Electrical and Computer Engineering, Kanazawa University, Ishikawa 920-1192, Japan (e-mail: maruyama@ec.t.kanazawa-u.ac.jp).

Color versions of one or more of the figures in this paper are available online at <http://ieeexplore.ieee.org>.

Digital Object Identifier 10.1109/JSTQE.2011.2128859

were achieved using SOI substrates [10]–[14]. As for modulators based on Si, a Mach–Zehnder interferometric modulator with a 3-dB cutoff frequency higher than 30 GHz [15], a four-channel wavelength division multiplexed microring modulator with a speed of 50 Gbit/s [16], a CMOS modulator with an optical pulse energy of 400 fJ/bit under a driving voltage of 1 V [17], and many more have been reported.

On the other hand, in the case of light sources based on Si or SOI substrates, the continuous wave (CW) operation of a Raman silicon laser was demonstrated under optical pumping [18]. Furthermore, a moderately low power consumption of 20 mW as well as a high differential quantum efficiency of 28% was achieved [19]. A direct gap transition from Ge-on-Si was also reported [20] and its CW operation under optical pumping was demonstrated at room temperature [21]. The RT-CW operation of injection-type III–V semiconductor lasers on Si substrates prepared by means of epitaxial growth and a wafer direct bonding method [22] were reported in the 1980s and 1990s at a wavelength of 1.3 [23] and 1.55  $\mu\text{m}$  [24]. Recently, long wavelength lasers grown on Si substrates were developed using GaSb [25] and Ga(NAsP) [26] compound semiconductors. Long wavelength injection lasers have also been prepared by benzocyclobutene (BCB) polymer bonding [27] and low temperature oxygen plasma-assisted bonding [28]. For the functional operation as well as the monolithic integration of these lasers on SOI waveguides, facet-free lasers evanescently coupled with Si waveguides were proposed [29]–[31]. Whereas most of these lasers have similar threshold currents and light output characteristics as conventional double-heterostructure lasers, an extremely low threshold current of less than 100  $\mu\text{A}$  was achieved with vertical-cavity surface-emitting lasers (VCSELs) [32] and micro-disk lasers [33]. The latter are characterized by the very small volume of the active region as well as high reflectivity mirrors (high Q cavities). Recently, BCB-bonded micro-disk lasers were reported and a threshold current as low as 0.35 mA was achieved [34]–[36]. A 2-D PC laser with a thin slab waveguide structure is another promising candidate for on-chip optical wiring. In particular, a threshold current of 0.23 mA can be achieved with a single cell PC laser [37]. An extremely low threshold operation and a fairly high differential quantum efficiency was reported under optical pumping for a 2-D PC-based short cavity laser with a thin (150 nm) slab waveguide structure emitting at 1.55  $\mu\text{m}$  wavelength [38]. Finally, a low pulse energy of 8.8 fJ/bit was achieved with a 20 Gbit/s nonreturn-to-zero (NRZ) signal [39].

In this paper, we present our approach to the development of low power consumption lasers with low threshold operation as well as high differential quantum efficiency, which could ultimately lead to the introduction of optical interconnects and on-chip optical wiring in future LSIs. First, we examined the use of strongly index-coupled grating lasers (DFB and distributed reflector (DR) lasers) characterized by a wire-like active region and then combined them with high index-contrast membrane waveguides to enhance the optical confinement in the active layer.

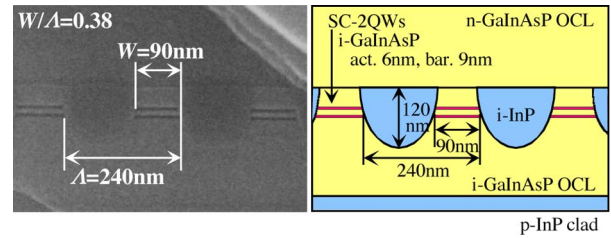


Fig. 1. Cross-sectional SEM view and schematic diagram of the structure of a DFB laser with a wire-like active region, where strain-compensated (SC) quantum wells (QWs) are sandwiched by GaInAsP optical confinement layers (OCLs).

## II. STRONGLY INDEX-COUPLED GRATING LASERS

### A. DFB Lasers With Wire-Like Active Regions

To realize a low threshold current operation, we proposed a DFB laser characterized by wire-like active regions, as shown in Fig. 1, which combines active regions of relatively small volume with a moderately high index-coupling coefficient  $\kappa_i$  of the grating. The maximum obtainable  $\kappa_i$  is approximately  $400\text{ cm}^{-1}$  for an active region buried in InP with width half of the grating period and an etched depth of 120 nm. Thanks to the inherent characteristics of GaInAsP/InP compounds and low-damage reactive ion etching (RIE) with a mixture of  $\text{CH}_4$  and  $\text{H}_2$  gases followed by wet chemical etching, the surface recombination velocity at the etched/regrown interface was estimated to be in the order of hundreds of centimeter per second. Therefore, the fraction of nonradiative recombination current to the total injection current can be reduced to approximately 5% for a wire width of 100 nm. A record low threshold current density of  $94\text{ A/cm}^2$  was obtained in the case of a  $20\text{ }\mu\text{m}$  wide mesa stripe device with twice as many quantum-well (DQW) wire-like active regions [40]. In the case of a buried heterostructure device with a wire width of 90 nm and a stripe width of  $2.3\text{ }\mu\text{m}$ , a submilliampere (0.7 mA) threshold current density was obtained under RT-CW conditions [41]. Due to the strong index coupling, the standing wave profile shifts toward the wire-like active region in the middle of the cavity. Hence, resonant modes on the longer wavelength side of the stopband are more pronounced than those on the shorter wavelength side. In other words, a more stable single-mode operation was achieved on the longer wavelength side of the stopband with very high yield for devices without phase-shift/phase-adjusted regions [42], [43]. Since this mode selection mechanism is different from that in gain- and complex-coupled DFB lasers, we called it “gain-matching effect” in strongly index-coupled grating structures.

### B. DR Lasers With Wire-Like Active Regions

A DR laser consisting of an active DFB section and a passive distributed Bragg reflector were proposed to achieve high differential quantum efficiency for the output of the DFB section without sacrificing the stable single-mode operation; hence, it is suitable for monolithically integrated photonic circuits [44]. When the width of the wire-like active regions becomes narrower than 50 nm, an energy blueshift due to the quantum size

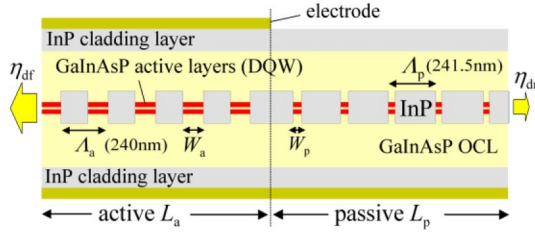
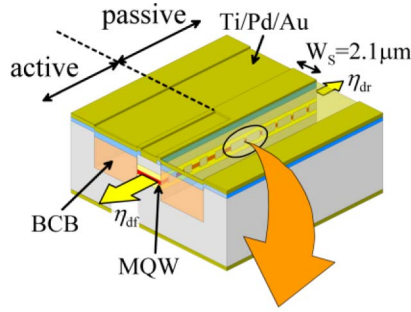


Fig. 2. Structure of a DR laser with wire-like active regions and its cross-sectional schematic diagram.

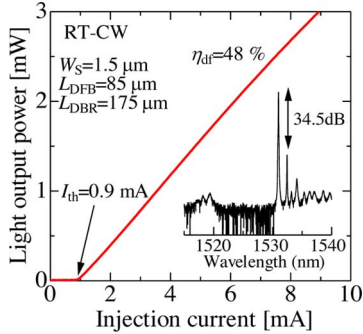


Fig. 3.  $IL$  characteristic of a DR laser with a  $\lambda/16$  phase shift at approximately  $40 \mu\text{m}$  from the front facet of the DFB section.

effect in the lateral direction becomes noticeable. By exploiting this effect and adopting different wire widths for the DFB and DBR section, as shown in Fig. 2, researchers were able to obtain DR lasers with relatively low threshold current and moderately high differential quantum efficiency [45], [46]. Recently, a threshold current of 0.9 mA and a differential quantum efficiency of 48% were achieved for the front facet when the DFB section length was set to  $85 \mu\text{m}$  and the stripe width to  $1.5 \mu\text{m}$ , as shown in Fig. 3 [47]. The threshold current density of these DR lasers was approximately 2–3 times higher than that of previously reported DFB lasers with similar active region width [41] that may be attributed to the quality of the initial wafer. The injection current for the 1 mW light output was estimated to be equal to 3.6 mA, which is, to the best of our knowledge, the lowest ever reported for all different types of edge-emitting single-mode lasers. Monolithic integration of a front-side power monitor using the less absorptive grating section of the slightly narrower wire-like active regions is also possible [46], [48]. High-speed modulation up to 10 Gbit/s [49] as well as low-power consumption was achieved in the case of 10 Gbit/s modulation when the bias current was up to 10 mA and

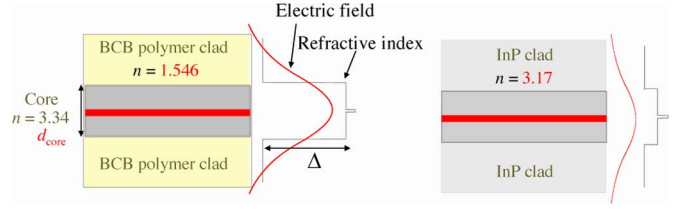


Fig. 4. Schematic diagram and optical field profile of a semiconductor membrane structure (left) and a conventional double-heterostructure (right).

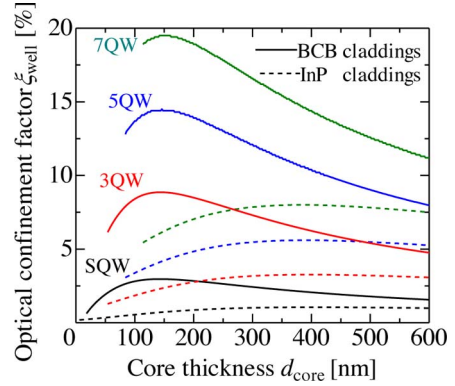


Fig. 5. Calculated 1-D optical confinement factors.

the modulation efficiency at approximately  $3 \text{ GHz}/\text{mA}^{1/2}$  [50]. However, the optical output power at so low bias current was a few milliwatt level and much low power consumption is required for high-speed modulation ( $>10 \text{ Gbit/s}$ ) in the case of on-chip optical wiring. On the other hand, the high optical feedback tolerance observed in DR lasers with wire-like active regions has been attributed to the strong mode selectivity that these lasers exhibit under stable single-mode operation; it can be potentially employed for on-chip optical wiring, where an isolator-free operation is preferable [51].

### III. SEMICONDUCTOR MEMBRANE LASERS

#### A. Membrane DFB Lasers With Wire-Like Active Regions

Since a typical semiconductor laser consists of multiple QWs (MQWs) acting as the active region sandwiched between wider band-gap semiconductor cladding layers with a refractive index approximately 5–10% lower than the refractive index of the active region, the optical confinement factor  $\xi$  of the active region in GaInAsP/InP long wavelength lasers is limited to approximately 1% per QW (for 6 nm thick and 1% compressively strained QW). When the InP cladding layers are replaced by low refractive index polymer such as BCB or  $\text{SiO}_2$ , the optical field is strongly confined into the semiconductor core layer, as shown in Fig. 4.

Fig. 5 shows the optical confinement factors for several MQW structures,  $\xi_{\text{well}}$ , as a function of the thickness of the semiconductor core layer,  $d_{\text{core}}$ . When BCB cladding layers are employed, it gradually increases with decreasing  $d_{\text{core}}$  and becomes maximum for  $d_{\text{core}} = 100\text{--}200 \text{ nm}$ . At the same time, the optical confinement factor per the number of MQWs is

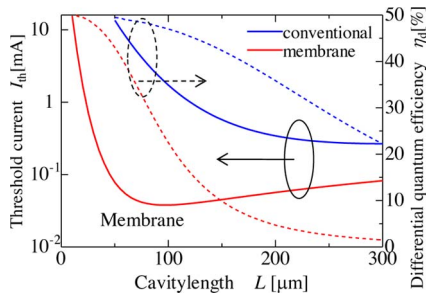


Fig. 6. Theoretical threshold current (normalized by the stripe width of 1  $\mu\text{m}$ ) and differential quantum efficiency as a function of the cavity length of membrane DFB laser (lower two curves) and conventional DFB laser (upper two curves).

increased by approximately three times (except in the case of SQWs) compared to that in conventional MQW lasers with InP cladding layers. Namely, three times higher modal gain can be attained with an active region of the same volume at the same injected carrier density. This enhancement is stronger than when the size of quantum wires used as an active region is controlled. In GaInAsP/InP lasers, the carrier lifetime is considered to be inversely proportional to the injected carrier density and a significantly lower threshold current can be attained if the threshold carrier density is reduced with the adoption of a semiconductor membrane structure.

Moreover, in the case of the membrane DFB lasers with wire-like active regions, the index-coupling coefficient  $\kappa_i$  of the grating can be enhanced by a factor of approximately 3 ( $\kappa_i = 1200 \text{ cm}^{-1}$ ). Therefore, the cavity length to obtain the same differential quantum efficiency (for the same coupling strength  $\kappa_i L$ ) can be shortened to 1/3 of cavity length in conventional DFB lasers with wire-like active regions. Fig. 6 shows the theoretical threshold current and the differential quantum efficiency for one facet (where the facet reflectivity is assumed to be 0, the active region width is half the grating period, and the number of QWs is 2) of a DFB laser with wire-like active regions as a function of the cavity length. As can be seen, a threshold current less than 50  $\mu\text{A}$  can be possible for a stripe with a width of 1  $\mu\text{m}$  without sacrificing the differential quantum efficiency [52], [53]. It should also be noted that this is almost one order of magnitude lower than that of the threshold current of the aforementioned DFB and DR lasers with wire-like active regions. If these lasers operated at 10 Gbit/s with a bias current of ten times the threshold (500  $\mu\text{A}$ ), the peak pulse power of approximately 100  $\mu\text{W}$  can be attained; hence, the optical pulse energy becomes 10 fJ/bit, which can meet the requirements for on-chip optical interconnection explained in Section I.

Since current injection-type membrane DFB lasers were beyond the capabilities of our fabrication technology, we attempted to prepare membrane DFB lasers for optical pumping by means of electron-beam lithography (EBL) followed by low-damage RIE with a mixture of  $\text{CH}_4$  and  $\text{H}_2$  gases and organometallic vapor-phase epitaxy (OMVPE) regrowth. Stable RT-CW operation was achieved for devices bonded with BCB on an InP substrate [52], [53]. Since the equivalent refractive index of this membrane structure is much lower (approximately 2.3 for a thickness of 150 nm) than that of conventional long

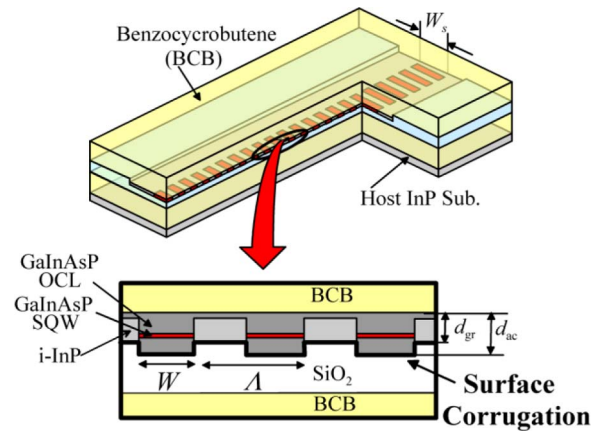


Fig. 7. Structure of a membrane DFB laser with surface corrugation grating and its cross-sectional schematic diagram.

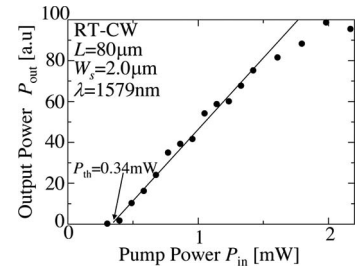


Fig. 8. Light output as a function of optical pump power of a membrane DFB laser with surface corrugation grating.

wavelength lasers, the grating period (first order) was set at approximately 315 nm. Even though the equivalent refractive index of this waveguide is sensitive with respect to the thickness, the lasing wavelength of the lasers prepared on an InP substrate deviated by only  $\pm 1.2 \text{ nm}$  from the average value. In addition, a laser array capable of covering multiple wavelengths (total range 75 nm) was obtained by varying both the grating period and the width of the active regions [54], [55]. By reducing the thickness of the membrane structure from 150 to 65 nm, the temperature coefficient of the lasing wavelength was reduced to  $2.45 \times 10^{-2} \text{ nm/deg}$ , which is approximately 20% lower than that of conventional GaInAsP/InP lasers, while that of InP was estimated to be  $2 \times 10^{-4} \text{ /deg}$ . This difference is attributed to the negative temperature coefficient ( $-7 \times 10^{-5} \text{ /deg}$ ) of the BCB cladding layer. [56].

In order to reduce the threshold current, membrane DFB lasers with surface corrugation grating (see Fig. 7) were fabricated by controlling the amount of InP grown on the groove region so as to obtain a relatively high index-coupling coefficient  $\kappa_i = 4200 \text{ cm}^{-1}$  for a surface corrugation depth of 40 nm. A threshold pump power  $P_{th}$  (980 nm wavelength pump light source) of 0.34 mW was obtained in the case of a device of 2  $\mu\text{m}$  width and 80  $\mu\text{m}$  length under RT-CW conditions, while the pump beam was of 4  $\mu\text{m}$  width and 176  $\mu\text{m}$  length, as shown in Fig. 8 [57]. Furthermore, the effective threshold pump power was estimated to be equal to 85  $\mu\text{W}$ , and corresponding threshold current 24  $\mu\text{A}$  under the assumption that the absorption coefficient for the pump light was  $10\,000 \text{ cm}^{-1}$ . A stable

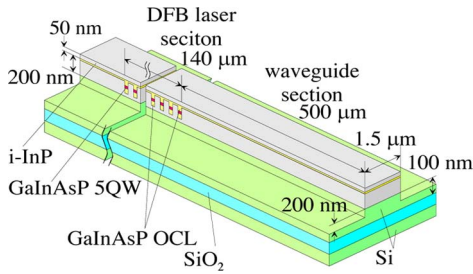


Fig. 9. Schematic diagram of the rib waveguide membrane DFB laser integrated with a passive waveguide fabricated on an SOI substrate.

single-mode operation with a submode suppression ratio of 35 dB was obtained at a pump power  $P = 2P_{th}$ . Since the operating power was very low compared with the area of the membrane DFB laser with BCB cladding layers, stable CW operation was maintained up to a temperature of 85 °C, which was the upper limit of the measurement setup, even though the thermal resistance of the structure seemed to be unusually high [58].

For the development of an optical platform for an optical wiring, not only in-plane integrations of active photonic components (at least lasers and detectors) and low-loss passive optical components but also electrical connections between the surface of an LSI chip and the active photonic components by using via holes are required, and severe requirements for very small footprint, high temperature operation capability, and so on will be imposed. For building up an optical layer, an integration of III–V compound active components on Si passive components (Si photonics) formed by matured CMOS technology is essential, and it can be done by BCB bonding or wafer direct bonding by using evanescent coupling [27]–[31] or by an integrated-twin-guide (ITG) structure [59], [60].

As a step to realize membrane-type lasers for in-plane photonic integration, we examined two different approaches. First, an air-bridge structure was prepared by etching a sacrificial layer beneath the membrane waveguide [61], an approach frequently adopted for 2-D PC devices. Even though the  $P_{th}$  was 13 times higher than that in [57], a stable CW operation was maintained up to a temperature of 80 °C. Second, we investigated the possibility of directly bonding a GaInAsP/InP membrane on an SOI substrate [62]. Specifically, a  $P_{th}$  of 2.8 mW was obtained for a device of 2 μm width and 120 μm length under RT-CW conditions [63]. Subsequently, a rib waveguide membrane DFB laser was integrated with a passive waveguide fabricated on an SOI substrate, as shown in Fig. 9 [64]. Due to the thickness of the waveguide, consisting of a 200 nm thick Si layer, a 200 nm thick GaInAsP/InP layer, and a 50 nm thick GaInAs layer, the CW operation was maintained up to a temperature of 85 °C (limited by the measurement setup). The optical coupling efficiency between the laser and the waveguide caused from a mismatch of the mode fields was estimated to be 99.5%. When the total thickness of the DFB laser structure is different from that of the waveguide, an adiabatic mode transformer or a tapered waveguide is required [65].

### B. Lateral Current Injection Lasers

Before their application as light sources in the on-chip optical wiring between LSIs would be possible, injection-type

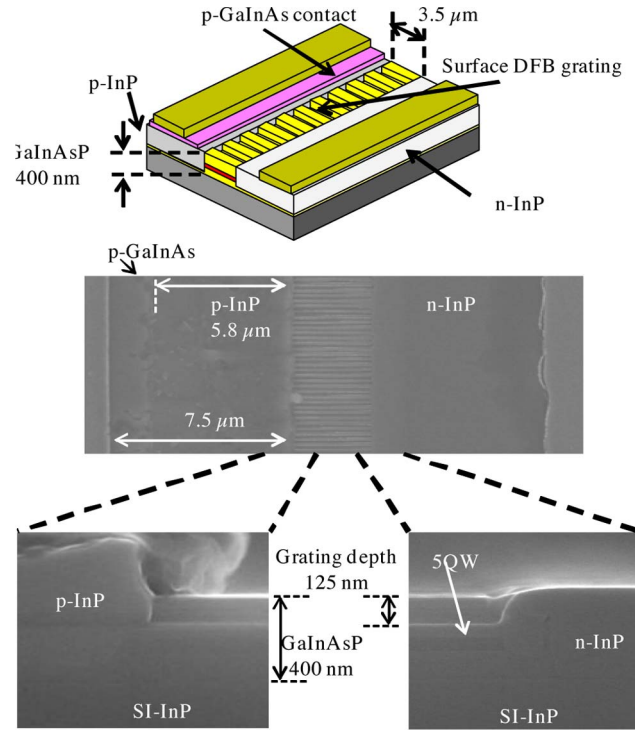


Fig. 10. Schematic diagram, top view, and cross-sectional SEM views of an LCI DFB laser grown on a SI InP substrate.

lasers with ultralow power consumption are required. As the first step toward the fabrication of an injection-type laser on a SOI substrate, various III–V lasers evanescently coupled to Si waveguides were examined [28]–[31]. We also developed an injection-type DFB laser with double-layered wire-like active regions bonded on an SOI substrate and obtained a threshold current density  $J_{th}$  of 400 A/cm<sup>2</sup> (threshold current  $I_{th}$  of 104 mA) for a stripe width of 25 μm and a cavity length of 1 mm [66].

Our next step was to develop an LCI structure [67] for our membrane DFB lasers. First, we grew a five-layer compressive strain MQWs (CS-MQWs) GaInAsP/InP wafer with a thickness of 400 nm on a semi-insulating (SI) InP substrate and, subsequently, formed surface grating with a depth of 125 nm. It should be noted that the MQW active layers were not etched to wire-like shape. Fig. 10 shows a schematic diagram along with top and cross-sectional SEM views of the device fabricated by a three-step OMVPE process [68]. A threshold current  $I_{th}$  of 27 mA was obtained for a stripe width of 3.5 μm and cavity length of 300 μm. Because the stripe width is significantly larger than the carrier diffusion length and the mobility of electrons higher than that of holes, relatively poor lasing characteristics were attributed to the nonuniform distribution of the injected carriers.

Therefore, we fabricated Fabry–Perot cavity lasers with a narrower stripe (width less than 2 μm) using the same initial wafer structure (with CS-MQWs and thickness of 400 nm) grown on an SI InP substrate [69], [70]. Fig. 11 shows cross-sectional structures of device (A) where a part of the lower GaInAsP optical confinement layer (OCL) is remained and device (B) where the lower GaInAsP OCL is completely etched. Since the active region (CS-MQWs) is sandwiched between upper and lower OCLs with 150-nm thick GaInAsP grown on an SI InP substrate and the peak of the optical field profile is observed

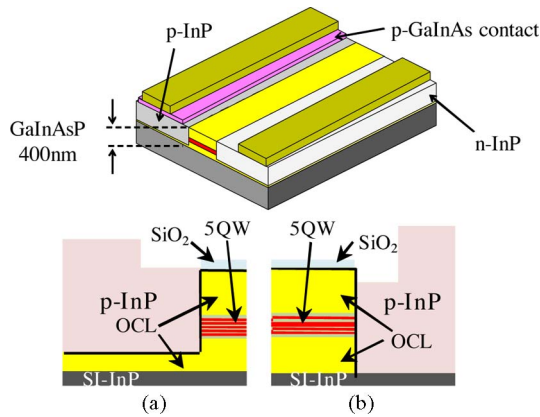


Fig. 11. Structure of LCI lasers grown on SI InP substrate; (A) lower OCL on SI InP was remained and (B) the OCL was completely etched.

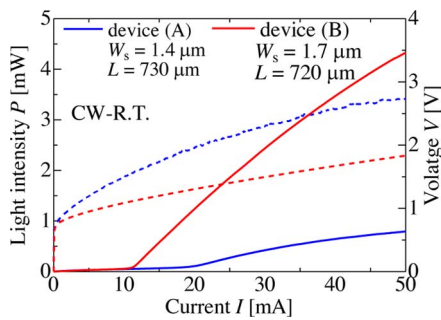


Fig. 12.  $IL$  and  $VI$  curves of the fabricated LCI laser.

below the CS-MQWs, the optical confinement factor  $\xi$  is estimated to be 5%. Fig. 12 shows the light output as well as the voltage–current ( $VI$ ) curves for these devices [68]. As can be seen,  $I_{th}$  of 11 mA (corresponding  $J_{th}$  of  $900 \text{ A/cm}^2$ ) and a differential quantum efficiency (for both facets) of 33% were obtained with device (B) with a stripe width of  $1.7 \mu\text{m}$  and a cavity length of  $720 \mu\text{m}$ . The waveguide loss and the internal quantum efficiency of device (B) were estimated based on the reciprocal dependence of the cavity length and the differential quantum efficiency to be  $4 \text{ cm}^{-1}$  and 40%, respectively, whereas they were equal to  $6 \text{ cm}^{-1}$  and 19% in the case of device (A). These differences are attributed to lower internal quantum efficiency in device (A) because a significant proportion of carrier recombination takes place near to the p-GaInAsP OCL due to lower mobility of holes than that of electrons.

Subsequently, we fabricated DFB lasers with almost the same cross-sectional structure (the active region consists of CS-MQWs, while the lower OCL is completely etched) based on device (B). Specifically, the DFB grating was formed by depositing 30-nm-thick amorphous Si on the stripe region by plasma-enhanced chemical vapor deposition followed by an EBL and inductively coupled  $\text{CF}_4$  plasma etching. The index-coupling coefficient  $\kappa_i$  of the surface grating was approximately  $100 \text{ cm}^{-1}$ . As a result,  $I_{th}$  of 7 mA (corresponding to  $J_{th}$  of  $1.17 \text{ kA/cm}^2$ ) and a differential quantum efficiency of 43% were obtained for the front facet of an as-cleaved device with a stripe width of  $2.0 \mu\text{m}$  and cavity length of  $300 \mu\text{m}$  [71]. In addition, a rise-up voltage of 0.8 V and a differential series resistance of  $25 \Omega$  were

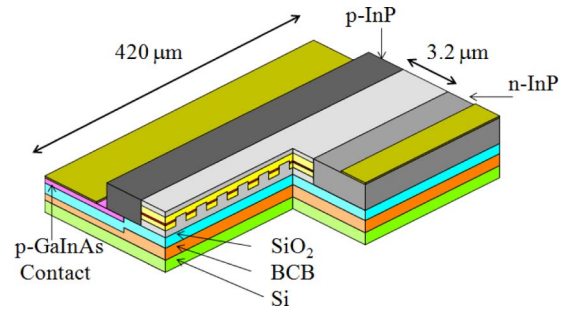


Fig. 13. Schematic diagram of the injection type membrane DFB laser with wire-like active regions.

obtained. Since a reduction of the stripe width leads to a reduction of not only the threshold current but also of the differential series resistance, higher performance is expected in narrower stripe devices. Since two steps of photolithography followed by an etching and OMVPE regrowth were employed in these works, the stripe width (approximately  $2 \mu\text{m}$ ) was limited by the alignment accuracy. It can be reduced by using an electron-exposure system with better alignment accuracy. Although the differential quantum efficiency of the rear facet was not accurately measured, it was estimated to be approximately 10–12% when the device was mounted on a submount for high-speed modulation. Based on these findings, the internal quantum efficiency was estimated to be 61–63% under the assumption that the waveguide loss is  $4\text{--}6 \text{ cm}^{-1}$ , namely 23–25% lower than that of the vertical injection-type GaInAsP/InP BH lasers with a stripe width of  $2.0 \mu\text{m}$  fabricated in our group.

Even though the internal quantum efficiency of LCI lasers was still poor when compared to that of conventional vertical current injection lasers, we tried to fabricate an injection-type membrane DFB laser with wire-like active regions, as shown in Fig. 13. The top and bottom cladding layers were composed of air ( $n = 1$ ) and  $\text{SiO}_2$  ( $n = 1.45$ ), respectively. The membrane core layer consists of 1% GaInAs CS-MQWs (90 nm thick, five 6-nm-thick wells well separated by six 10-nm-thick barriers) sandwiched between GaInAsP OCLs ( $\lambda_g = 1200 \text{ nm}$  and 165 nm thick) and 50-nm-thick InP cap layers; namely, the total thickness of the membrane core layer is 470 nm. The grating period and the active region width were 255 and 110 nm, respectively, while  $\kappa_i$  of this grating with a depth of 190 nm was estimated to be  $550 \text{ cm}^{-1}$ . After completing the fabrication of the lateral PIN junction stripe structure, a  $1\text{-}\mu\text{m}$ -thick  $\text{SiO}_2$  and a  $2\text{-}\mu\text{m}$ -thick BCB layer were deposited and spin coated, respectively. Next, the wafer was bonded upside down on an SOI host substrate, and the BCB hard baked at a temperature of  $250^\circ\text{C}$  for 1 h in  $\text{N}_2$  environment. Finally, the InP substrate and etch-stop layers were removed by polishing and wet chemical etching, and Ti/Au electrodes were deposited on both the p-GaInAs contact and n-InP sections. A threshold current of 83 mA and an external differential quantum efficiency of 1.1% were obtained for a stripe width of  $3.2 \mu\text{m}$  and cavity length of  $420 \mu\text{m}$  under RT-pulsed operation [72]. The differential series resistance was estimated to be  $46 \Omega$ , which was approximately two times higher than that of LCI-DFB lasers with a Si grating.

In spite of the relatively high optical confinement factor (1.9% per well) compared with that previously reported for LCI lasers (1% per well) [70], [71], and the DFB cavity characterized by high  $\kappa_i$ , the poor performance may be due to the BCB bonding process during which air voids were trapped within the bonding interface and caused bending of the membrane structure or cracks, resulting in relatively large scattering loss within the cavity. Consequently, further improvements in the BCB bonding process or the introduction of an air-bridge structure are being investigated to overcome the shortcomings.

#### IV. CONCLUSION

Recent advancements in the fabrication of long-wavelength GaInAsP/InP lasers with low power consumption are reviewed. While DFB and DR lasers with wire-like active regions can be promising light sources for in-plane photonic integrated circuits with output power of a few hundreds microwatt to 1 mW level, membrane lasers are also a promising alternative for achieving even lower power consumption. Their most attractive characteristic is the enhancement of not only the optical confinement factor of the active region but also of the index-coupling coefficient of the grating. The low power consumption was confirmed for optically pumped membrane DFB lasers under CW conditions up to a moderately high temperature of 85 °C. Next, an LCI structure was investigated for injection-type membrane lasers with low power consumption, and LCI-Fabry–Perot and LCI-DFB lasers were prepared on SI InP substrates. The threshold current and differential quantum efficiency of the latter were satisfactory even though the internal quantum efficiency of these LCI lasers was found to be slightly poorer than that of conventional vertical injection-type BH lasers. Consequently, further improvements in the structure and fabrication process of LCI membrane lasers are being investigated.

#### ACKNOWLEDGMENT

The authors would like to thank Prof. E. Y. Suematsu, Prof. K. Iga, Prof. K. Kobayashi, and Prof. K. Furuya for their continuous encouragement, and Prof. M. Asada, Prof. F. Koyama, Prof. T. Mizumoto, Prof. Y. Miyamoto, and Dr. S. Lee of the Tokyo Institute of Technology for the fruitful discussions. They also like to acknowledge the contribution of all former/present students who participated in the exhaustive investigations of low-damage fabrication processes of ultrafine structures for GaInAsP/InP long wavelength quantum-wire lasers and related photonic devices since the 1980s.

#### REFERENCES

- [1] D. A. B. Miller, "Rationale and challenges for optical interconnects to electronic chips," *Proc. IEEE*, vol. 88, no. 6, pp. 728–749, Jun. 2000.
- [2] J. Ahn, M. Fiorentino, R. G. Beausoleil, N. Binkert, A. Davis, D. Fattal, N. P. Jouppi, M. McLaren, C. M. Santori, R. S. Schreiber, S. M. Spillane, D. Vantrease, and Q. Xu, "Devices and architectures for photonic chip-scale integration," *Appl. Phys. A*, vol. 95, no. 4, pp. 989–997, Feb. 2009.
- [3] I. A. Young, E. Mohammed, J. T. S. Liao, A. M. Kern, S. Palermo, B. A. Block, M. R. Reshotko, and P. L. D. Chang, "Optical I/O technology for tera-scale computing," *IEEE J. Solid-State Circuits*, vol. 45, no. 1, pp. 235–248, Jan. 2010.

- [4] M. Paniccia, "Integrating silicon photonics," *Nat. Photon.*, vol. 4, pp. 498–499, Aug. 2010.
- [5] R. Soref, "The past, present, and future of silicon photonics," *IEEE J. Sel. Topics Quantum Electron.*, vol. 12, no. 6, pp. 1678–1687, Nov./Dec. 2006.
- [6] L. C. Kimerling, D. Ahn, A. B. Apsel, M. Beals, D. Carothers, Y.-K. Chen, T. Conway, D. M. Gill, M. Grove, C.-Y. Hong, M. Lipson, J. Liu, J. Michel, D. Pan, S. S. Patel, A. T. Pomerene, M. Rasras, D. K. Sparacin, K.-Y. Tu, A. E. White, and C. W. Wong, "Electronic-photonic integrated circuits on the CMOS platform," *Proc. SPIE*, vol. 6125, pp. 612502-1–612502-10, Jan. 2006.
- [7] Y. A. Vlasov and S. J. McNab, "Losses in single-mode silicon-on-insulator strip waveguides and bends," *Opt. Exp.*, vol. 12, no. 8, pp. 1622–1631, Apr. 2004.
- [8] T. Asano, B. S. Song, and S. Noda, "Analysis of the experimental Q factors ( $\sim 1$  million) of photonic crystal nanocavities," *Opt. Exp.*, vol. 14, no. 5, pp. 1996–2002, Mar. 2006.
- [9] J. Rattner, "The mega-center," *Intel Developer Forum*, Mar. 2006.
- [10] M. Rouviere, L. Vivien, X. Le Roux, J. Mangeney, P. Crozat, C. Hoarau, E. Cassan, D. Pascal, and S. Laval, "Ultrahigh speed germanium-on-silicon-on-insulator photodetectors for 1.31 and 1.55  $\mu\text{m}$  operation," *Appl. Phys. Lett.*, vol. 87, pp. 231109-1–231109-3, Nov. 2005.
- [11] T. Yin, R. Cohen, M. M. Morse, G. Sarid, Y. Chetrit, D. Rubin, and M. J. Paniccia, "31GHz Ge n-i-p waveguide photodetectors on silicon-on-insulator substrate," *Opt. Exp.*, vol. 15, no. 21, pp. 13965–13971, Oct. 2007.
- [12] Y. Kang, H. D. Liu, M. Morse, M. J. Paniccia, M. Zadka, S. Litski, G. Sarid, A. Pauchard, Y. H. Kuo, H. W. Chen, W. S. Zaoui, J. E. Bowers, A. Beling, D. C. McIntosh, X. Zheng, and J. C. Campbell, "Monolithic germanium/silicon avalanche photodiodes with 340 GHz gain-bandwidth product," *Nat. Photon.*, vol. 3, pp. 59–63, Dec. 2008.
- [13] L. Vivien, J. Osmond, J. M. Fédéli, D. M. Morini, P. Crozat, J. F. Damlencourt, E. Cassan, Y. Lecunff, and S. Laval, "42 GHz p-i-n germanium photodetector integrated in a silicon-on-insulator waveguide," *Opt. Exp.*, vol. 17, no. 8, pp. 6252–6257, Apr. 2009.
- [14] P. R. A. Binetti, X. J. M. Leijtens, T. de Vries, Y. S. Oei, L. Di Cioccio, J.-M. Fedeli, C. Lagahe, J. Van Campenhout, D. Van Thourhout, P. J. van Veldhoven, R. Nötzel, and M. K. Smit, "InP/InGaAs photodetectors on SOI circuitry," in *Proc. Int. Conf. Group IV Photonics*. San Francisco, CA, , pp. 214–216, Paper FA7.
- [15] L. Liao A. Liu, D. Rubin, J. Basak, Y. Chetrit, H. Nguyen, R. Cohen, N. Izhaky, and M. Paniccia, "40 Gbit/s silicon optical modulator for high-speed applications," *Electron. Lett.*, vol. 43, no. 22, pp. 1196–1197, Oct. 2007.
- [16] S. Manipartruni, C. Long Chen, and M. Lipson, "50 Gbit/s wavelength division multiplexing using silicon microring modulators," in *Proc. Int. Conf. Group IV Photonics*. vol. FC3, San Francisco, CA, Sep. 2009, pp. 244–246, Paper FC3.
- [17] X. e. Zheng, J. Lexau, Y. Luo, H. Thacker, T. Pinguet, A. Mekis, G. Li, J. Shi, P. Amberg, N. Pinckney, K. Raj, R. Ho, J. E. Cunningham, and A. V. Krishnamoorthy, "Ultra-low-energy all-CMOS modulator integrated with driver," *Opt. Exp.*, vol. 18, no. 3, pp. 3059–3070, Feb. 2010.
- [18] H. Rong, R. Jones, A. Liu, O. Cohen, D. Hak, A. Fang, and M. Paniccia, "A continuous-wave Raman silicon laser," *Nature*, vol. 433, no. 7027, pp. 725–728, Feb. 2005.
- [19] H. Rong, S. Xu, Y.-H. Kuo, V. Sih, O. Cohen, O. Raday, and M. Paniccia, "Low-threshold continuous-wave Raman silicon laser," *Nat. Photon.*, vol. 1, no. 4, pp. 232–237, Apr. 2007.
- [20] J. Liu, S. Xiaochen, L. C. Kimerling, and J. Michel, "Optical gain from the direct gap transition of Ge-on-Si at room temperature," in *Proc. Int. Conf. Group IV Photonics*. San Francisco, CA, Sep. 2009, pp. 262–264, Paper FD2.
- [21] J. Liu, X. Sun, R. C.-Aguilera, L. C. Kimerling, and J. Michel, "Ge-on-Si laser operating at room temperature," *Opt. Lett.*, vol. 35, no. 5, pp. 679–681, Mar. 2010.
- [22] H. Wada and T. Kamijoh, "Room-temperature CW operation of InGaAsP lasers on Si fabricated by wafer bonding," *IEEE Photon. Technol. Lett.*, vol. 8, no. 2, pp. 173–175, Feb. 1996.
- [23] M. Razeghi, M. Defour, R. Blondeau, F. Omnes, P. Maurel, O. Acher, F. Brillouet, J. C. C. Fan, and J. Salerno, "First CW operation of a  $\text{Ga}_{0.25}\text{In}_{0.75}\text{As}_{0.5}\text{P}_{0.5}$ -InP laser on a silicon substrate," *Appl. Phys. Lett.*, vol. 53, no. 24, pp. 2389–2390, Dec. 1988.
- [24] M. Sugo, H. Mori, M. Tachikawa, Y. Itoh, and M. Yamamoto, "Room-temperature operation of an InGaAsP double-heterostructure laser emitting at 1.55  $\mu\text{m}$  on a Si substrate," *Appl. Phys. Lett.*, vol. 57, no. 6, pp. 593–595, Aug. 1990.

- [25] L. Cerutti, J. B. Rodríguez, and E. Tournie, "GaSb-based laser, monolithically grown on silicon substrate, emitting at 1.55  $\mu\text{m}$  at room temperature," *IEEE Photon. Technol. Lett.*, vol. 22, no. 8, pp. 553–555, Apr. 2010.
- [26] S. Liebich, M. Zimprich, P. Ludewig, A. Beyer, K. Volz, W. Stolz, B. Kunert, N. Hossain, S. R. Jin, and S. J. Sweeney, "MOVPE growth and characterization of Ga(NAsP) laser structures monolithically integrated on Si (0 0 1) substrates," in *Proc. IEEE 22nd Int. Semicond. Laser Conf.*, Kyoto, Japan, Sep. 2010, pp. 143–144, Paper WA5.
- [27] G. Roelkens, D. Van Thourhout, R. Baets, R. Nötzel, and M. Smit, "Laser emission and photodetection in an InP-InGaAsP layer integrated on and coupled to a silicon-on-insulator waveguide circuit," *Opt. Exp.*, vol. 14, no. 18, pp. 8154–8159, Sep. 2006.
- [28] A. W. Fang, H. Park, O. Cohen, R. Jones, M. J. Paniccia, and J. E. Bowers, "Electrically pumped hybrid AlGaInAs-silicon evanescent laser," *Opt. Exp.*, vol. 14, no. 20, pp. 9203–9210, Oct. 2006.
- [29] A. W. Fang, R. Jones, H. Park, O. Cohen, O. Raday, M. J. Paniccia, and J. E. Bowers, "Integrated AlGaInAs-Silicon evanescent race track laser and photodetector," *Opt. Exp.*, vol. 15, no. 5, pp. 2315–2322, Mar. 2007.
- [30] A. W. Fang, R. Jones, H. Park, O. Cohen, O. Raday, M. J. Paniccia, and J. E. Bowers, "A distributed feedback silicon evanescent laser," *Opt. Exp.*, vol. 16, no. 7, pp. 4413–4419, Mar. 2008.
- [31] D. Liang, M. Fiorentino, T. Okumura, H. H. Chang, D. T. Spencer, Y. H. Kuo, A. W. Fang, D. Dai, R. G. Beausoleil, and J. E. Bowers, "Electrically-pumped compact hybrid silicon microring lasers for optical interconnects," *Opt. Exp.*, vol. 17, no. 22, pp. 20355–20364, Oct. 2009.
- [32] K. Iga, "Surface emitting laser—Its birth and generation of new optoelectronics field," *IEEE J. Sel. Topics Quantum Electron.*, vol. 6, no. 6, pp. 1201–1215, Nov./Dec. 2000.
- [33] M. Fujita, R. Ushigome, and T. Baba, "Continuous wave lasing in GaInAsP microdisk injection laser with threshold current of 40  $\mu\text{A}$ ," *Electron. Lett.*, vol. 36, no. 9, pp. 790–791, Apr. 2000.
- [34] J. Van Campenhout, P. R. Romeo, P. Regreny, C. Seassal, D. V. Thourhout, S. Verstuyft, L. Di Cioccio, J.-M. Fedeli, C. Lagahe, and R. Baets, "Electrically pumped InP-based microdisk lasers integrated with a nanophotonic silicon-on-insulator waveguide circuit," *Opt. Exp.*, vol. 15, no. 11, pp. 6744–6749, May 2007.
- [35] J. V. Campenhout, P. R. A. Binetti, P. R. Romeo, P. Regreny, C. Seassal, X. J. M. Leijtsens, T. de Vries, Y. S. Oei, R. P. J. van Veldhoven, R. Nötzel, L. D. Cioccio, J. M. Fedeli, M. K. Smit, D. V. Thourhout, and R. Baets, "Low-footprint optical interconnect on an SOI chip through heterogeneous integration of InP-based microdisk lasers and microdetectors," *Opt. Exp.*, vol. 21, no. 8, pp. 522–524, Apr. 2009.
- [36] T. Spuesens, L. Liu, T. de Vries, P. R. Romeo, P. Regreny, and D. Van Thourhout, "Improved design of an InP-based microdisk laser heterogeneously integrated with SOI," in *Proc. Int. Conf. Group IV Photon.*, San Francisco, CA, Sep. 2009, pp. 202–204, Paper FA3.
- [37] H.-G. Park, S.-H. Kim, S.-H. Kwon, Y.-G. Ju, J.-K. Yang, J.-H. Baek, S.-B. Kim, and Y.-H. Lee, "Electrically driven single-cell photonic crystal laser," *Science*, vol. 305, no. 9, pp. 1444–1447, Sep. 2004.
- [38] S. Matsuo, A. Shinya, T. Kakitsuka, K. Nozaki, T. Segawa, T. Sato, Y. Kawaguchi, and M. Notomi, "High-speed ultracompact buried heterostructure-photonic-crystal laser with 13 fJ of energy consumed per bit transmitter," *Nat. Photon.*, vol. 4, pp. 648–654, Sep. 2010.
- [39] S. Matsuo, A. Shinya, C. H. Chen, K. Nozaki, T. Sato, Y. Kawaguchi, and M. Notomi, "20 Gbit/s directly modulated buried hetero-structure photonic crystal laser with 8.76-fJ/bit operating energy," presented at the European Conf. on Optical Commun., Torino, Italy, Sep. 2010, PaperPD1.6.
- [40] M. Nakamura, N. Nunoya, H. Yasumoto, M. Morshed, K. Fukuda, S. Tamura, and S. Arai, "Very low threshold current density operation of 1.5  $\mu\text{m}$  DFB lasers with wire-like active regions," *Electron. Lett.*, vol. 36, no. 7, pp. 639–640, Apr. 2000.
- [41] N. Nunoya, M. Nakamura, H. Yasumoto, M. Morshed, K. Fukuda, S. Tamura, and S. Arai, "Sub-milliampere operation of 1.5  $\mu\text{m}$  wavelength high index-coupled buried heterostructure distributed feedback lasers," *Electron. Lett.*, vol. 36, no. 14, pp. 1213–1214, Jul. 2000.
- [42] N. Nunoya, M. Nakamura, M. Morshed, S. Tamura, and S. Arai, "High-performance 1.55  $\mu\text{m}$  wavelength GaInAsP-InP distributed-feedback lasers with wire-like active regions," *IEEE J. Sel. Topics Quantum Electron.*, vol. 7, no. 2, pp. 249–258, Jun. 2001.
- [43] K. Ohira, N. Nunoya, and S. Arai, "Stable single-mode operation of distributed feedback lasers with wire-like active regions," *IEEE J. Sel. Topics Quantum Electron.*, vol. 9, no. 5, pp. 1166–1171, Sep./Oct. 2003.
- [44] J. I. Shim, K. Komori, S. Arai, I. Arima, Y. Suematsu, and R. Somchai, "Lasing characteristics of 1.5  $\mu\text{m}$  GaInAsP-InP SCH-BIG-DR lasers," *IEEE J. Quantum Electron.*, vol. 27, no. 6, pp. 1736–1745, Jun. 1991.
- [45] K. Ohira, T. Murayama, S. Tamura, and S. Arai, "Low-threshold and high-efficiency operation of distributed reflector lasers with width-modulated wire-like active regions," *IEEE J. Sel. Topics Quantum Electron.*, vol. 11, no. 5, pp. 1162–1168, Sep./Oct. 2005.
- [46] S. M. Ullah, S. H. Lee, R. Suemitsu, N. Nishiyama, and S. Arai, "GaInAsP/InP distributed reflector lasers and integration of front power monitor by using lateral quantum confinement effect," *Jpn. J. Appl. Phys.*, vol. 47, no. 6, pp. 4558–4565, Jun. 2008.
- [47] T. Shindo, S. Lee, D. Takahashi, N. Tajima, N. Nishiyama, and S. Arai, "Low-threshold and high-efficiency operation of distributed reflector laser with wire-like active regions," *IEEE Photon. Technol. Lett.*, vol. 21, no. 19, pp. 1414–1416, Oct. 2009.
- [48] S.-H. Lee, R. Suemitsu, S. M. Ullah, M. Otake, N. Nishiyama, and S. Arai, "Very high electric isolation between distributed reflector laser and front power monitor through deeply etched narrow groove," *Jpn. J. Appl. Phys.*, vol. 46, no. 39, pp. L954–L956, Oct. 2007.
- [49] S.-H. Lee, S. M. Ullah, T. Shindo, K. Davis, N. Nishiyama, and S. Arai, "Bit-error-rate measurement of GaInAsP/InP distributed reflector laser with wire-like active regions," presented at the 20th Int. Conf. Indium Phosphide and Related Materials, Versailles, May 2008.
- [50] D. Takahashi, S.-H. Lee, T. Shindo, K. Shinno, N. Nishiyama, and S. Arai, "Low-power consumption and high-eye-margin 10 Gbit/s operation of distributed reflector laser with wirelike active regions," to be presented at the 23rd Int. Conf. Indium Phosphide and Related Materials, Berlin, Germany, E2-3, May 2011.
- [51] S.-H. Lee, N. Tajima, T. Shindo, D. Takahashi, N. Nishiyama, and S. Arai, "High optical-feedback tolerance of distributed reflector lasers with wire-like active regions for isolator-free operation," *IEEE Photon. Technol. Lett.*, vol. 21, no. 20, pp. 1529–1531, Oct. 2009.
- [52] T. Okamoto, N. Nunoya, Y. Onodera, S. Tamura, and S. Arai, "Low-threshold single-mode operation of membrane BH-DFB lasers," *Electron. Lett.*, vol. 38, no. 23, pp. 1444–1446, Nov. 2002.
- [53] T. Okamoto, N. Nunoya, Y. Onodera, T. Yamazaki, S. Tamura, and S. Arai, "Optically pumped membrane BH-DFB lasers for low-threshold and single-mode operation," *IEEE J. Sel. Topics Quantum Electron.*, vol. 9, no. 5, pp. 1361–1366, Sep./Oct. 2003.
- [54] T. Okamoto, T. Yamazaki, S. Sakamoto, S. Tamura, and S. Arai, "Low-threshold membrane BH-DFB laser arrays with precisely controlled wavelength over a wide range," *IEEE Photon. Technol. Lett.*, vol. 16, no. 5, pp. 1242–1244, May 2004.
- [55] S. Sakamoto, T. Okamoto, T. Yamazaki, S. Tamura, and S. Arai, "Multiple-wavelengths membrane BH-DFB laser arrays," *IEEE J. Sel. Topics Quantum Electron.*, vol. 11, no. 5, pp. 1174–1179, Sep./Oct. 2005.
- [56] S. Sakamoto, H. Kawashima, H. Naitoh, S. Tamura, T. Maruyama, and S. Arai, "Reduced temperature dependence of lasing wavelength in membrane buried hetero-structure DFB lasers with polymer cladding layers," *IEEE Photon. Technol. Lett.*, vol. 19, no. 5, pp. 291–293, Mar. 2007.
- [57] S. Sakamoto, H. Naitoh, H. Kawashima, M. Ohtake, Y. Nishimoto, S. Tamura, T. Maruyama, N. Nishiyama, and S. Arai, "Strongly index-coupled membrane BH-DFB lasers with surface corrugation grating," *IEEE J. Sel. Topics Quantum Electron.*, vol. 13, no. 5, pp. 1135–1141, Sep./Oct. 2007.
- [58] S. Sakamoto, H. Naitoh, M. Ohtake, Y. Nishimoto, T. Maruyama, N. Nishiyama, and S. Arai, "85  $^{\circ}\text{C}$  continuous-wave operation of GaInAsP/InP-membrane buried heterostructure distributed feedback lasers with polymer cladding layer," *Jpn. J. Appl. Phys.*, vol. 46, no. 47, pp. L1155–L1157, Nov. 2007.
- [59] Y. Suematsu, M. Yamada, and K. Hayashi, "Integrated twin-guide AlGaAs laser with multiheterostructure," *IEEE J. Quantum Electron.*, vol. 11, no. 7, pp. 457–460, Jul. 1975.
- [60] T. Dupont, L. Grenouillet, A. Chelnokov, and P. Viktorovitch, "Contradirectional coupling between III–V stacks and silicon on-insulator corrugated waveguides for laser emission by distributed feedback effect," *IEEE Photon. Technol. Lett.*, vol. 22, no. 19, pp. 1413–1415, Oct. 2010.
- [61] H. Naitoh, S. Sakamoto, M. Ohtake, T. Okumura, T. Maruyama, N. Nishiyama, and S. Arai, "GaInAsP/InP membrane BH-DFB laser with air-bridge structure," *Jpn. J. Appl. Phys.*, vol. 46, no. 47, pp. L1158–L1160, Nov. 2007.
- [62] T. Maruyama, T. Okumura, and S. Arai, "Direct wafer bonding of GaInAsP/InP membrane structure on silicon-on-insulator substrate," *Jpn. J. Appl. Phys.*, vol. 45, no. 11, pp. 8717–8718, Nov. 2006.
- [63] T. Maruyama, T. Okumura, S. Sakamoto, K. Miura, Y. Nishimoto, and S. Arai, "GaInAsP/InP Membrane BH-DFB lasers directly bonded on

- SOI substrate,” *Opt. Exp.*, vol. 14, no. 18, pp. 8184–8188, Sep. 2006.
- [64] T. Okumura, T. Maruyama, M. Kanemaru, S. Sakamoto, and S. Arai, “Single-mode operation of GaInAsP/InP- membrane distributed feedback lasers bonded on silicon-on-insulator substrate with rib-waveguide structure,” *Jpn. J. Appl. Phys.*, vol. 46, no. 48, pp. 1206–1208, Dec. 2007.
- [65] B. Ben Bakir, N. Olivier, Ph. Grosse, S. Messaoudène, S. Brision, E. Augendre, P. Philippe, K. Gilbert, D. Bordel, J. Harduin, and J.-M. Fedeli, “Electrically driven hybrid Si/III–V lasers based on adiabatic mode transformers,” *Proc. SPIE*, vol. 7719, pp. 77191F-1–77191F-9, Apr. 2010.
- [66] T. Okumura, T. Maruyama, H. Yonezawa, N. Nishiyama, and S. Arai, “Injection-type GaInAsP-InP-Si distributed-feedback laser directly bonded on silicon-on-insulator substrate,” *IEEE Photon. Technol. Lett.*, vol. 21, no. 5, pp. 283–285, Mar. 2009.
- [67] K. Oe, Y. Noguchi, and C. Cannau, “GaInAsP Laterall Current Injection lasers on Semi-insulating Substrates,” *IEEE Photon. Technol. Lett.*, vol. 6, no. 4, pp. 479–481, Apr. 1994.
- [68] T. Okumura, M. Kurokawa, D. Kondo, H. Ito, N. Nishiyama, T. Maruyama, and S. Arai, “Lateral current injection type GaInAsP/InP DFB lasers on SI-InP substrate,” presented at the 21st Int. Conf. Indium Phosphide and Related Materials, Newport Beach, May 2009, Paper TuB2.5.
- [69] T. Okumura, M. Kurokawa, M. Shirao, D. Kondo, H. Ito, N. Nishiyama, T. Maruyama, and S. Arai, “Lateral current injection GaInAsP/InP laser on semi-insulating substrate for membrane-based photonic circuits,” *Opt. Exp.*, vol. 17, no. 15, pp. 12564–12570, Jul. 2009.
- [70] T. Okumura, H. Ito, D. Kondo, N. Nishiyama, and S. Arai, “Continuous wave operation of thin film lateral current injection lasers grown on semi-insulating InP substrates,” *Jpn. J. Appl. Phys.*, vol. 49, no. 4, pp. 040205-1–040205-3, Apr. 2010.
- [71] T. Shindo, Okumura, T. Koguchi, H. Ito, N. Nishiyama, and S. Arai, “First lasing operation of injection type membrane GaInAsP DFB laser with lateral current injection BH structure,” in presented at the 23rd Annu. Photon. Soc. Meeting, Denver, CO, Nov. 2010, Paper ThR4.
- [72] T. Okumura, T. Koguchi, H. Ito, N. Nishiyama, and S. Arai, “First lasing operation of injection type membrane GaInAsP DFB laser with lateral current injection BH structure,” in presented at the 22nd IEEE Int. Semicond. Laser Conf., Kyoto, Japan, Sep. 2010, Paper WA2.



**Shigehisa Arai** (M’83–SM’06–F’10) was born in Kanagawa prefecture, Japan, in 1953. He received the B.E., M.E., and D.E. degrees in electronics from the Tokyo Institute of Technology, Tokyo, Japan, in 1977, 1979, and 1982, respectively. During his Ph.D. study, he demonstrated room-temperature continuous wave (CW) operations of 1.11–1.67  $\mu\text{m}$  long-wavelength lasers fabricated by a liquid-phase epitaxy as well as their single-mode operations under a rapid direct modulation.

He joined the Department of Physical Electronics, Tokyo Institute of Technology, as a Research Associate in 1982, and joined AT&T Bell Laboratories, Holmdel, NJ, as a Visiting Researcher from 1983 to 1984, on leave from the Tokyo Institute of Technology. He became a Lecturer in 1984, an Associate Professor in 1987, and a Professor in the Research Center for Quantum Effect Electronics and the Department of Electrical and Electronic Engineering in 1994. Since 2004, he has been a Professor with the Quantum Nanoelectronics Research Center (QNERC), Tokyo Institute of Technology. His research interests include photonic integrated devices such as dynamic-single-mode and wavelength-tunable semiconductor lasers, semiconductor optical amplifiers, and optical switches/modulators. His current research interests include studies on low-damage and cost-effective processing technologies of ultrafine structures for high-performance lasers and photonic integrated circuits on silicon platforms.

Dr. Arai is a member of the Optical Society of America, the Institute of Electronics, Information, and Communication Engineers (IEICE), and the Japan Society of Applied Physics (JSAP). He received the Excellent Paper Award from the IEICE of Japan in 1988, the Michael Lunn Memorial Award from the Indium Phosphide and Related Materials Conference in 2000, Prizes for Science and Technology including a Commendation for Science and Technology from the Ministry of Education, Culture, Sports, Science, and Technology, Japan, in 2008, the Electronics Society Award from IEICE in 2008, and a JSAP Fellowship in 2008.



**Nobuhiko Nishiyama** (M’01–SM’07) was born in Yamaguchi prefecture, Japan, in 1974. He received the B.E., M.E., and Ph.D. degrees from the Tokyo Institute of Technology, in 1997, 1999 and 2001, respectively. During his Ph.D. study, he demonstrated single-mode 0.98 and 1.1  $\mu\text{m}$  vertical-cavity surface-emitting laser (VCSEL) arrays with stable polarization using misoriented substrates for high-speed optical networks as well as MOCVD-grown GaInNAs VCSELs.

He joined Corning, Inc., Corning, NY, in 2001 and was with the Semiconductor Technology Research Group. At Corning, Inc., he was involved in several subjects including short-wavelength lasers, 1060-nm DFB/DBR lasers, and long-wavelength InP-based VCSELs, demonstrating state-of-the-art results such as 10-Gbit/s isolator-free and high-temperature operations of long-wavelength VCSELs. Since 2006, he has been an Associate Professor at the Tokyo Institute of Technology. His current research interests include laser transistors, silicon-photonics, III–V silicon hybrid optical devices, and THz-optical signal conversions involving optics-electronics-radio integration circuits.

Dr. Nishiyama received the Excellent Paper Award from the Institute of Electronics, Information, and Communication Engineers (IEICE) of Japan in 2001 and the Young Scientists Prize in the Commendation for Science and Technology from the Ministry of Education, Culture, Sports, Science, and Technology in 2009. He is a member of the Japan Society of Applied Physics and IEICE.



**Takeo Maruyama** (M’08) was born in Toyama, Japan, in 1972. He received the B.E. degree in electrical and electronic engineering, and the M.E. and Ph.D. degrees in physical electronics all from the Tokyo Institute of Technology, Tokyo, Japan, in 1997, 1999, and 2002, respectively.

He became a Research Associate at the Research Center for Quantum Effect Electronics, Tokyo Institute of Technology in 2002, where he carried out research on the development of semiconductor membrane lasers on silicon substrates based on direct bonding. Since 2008, he has been with the School of Electrical and Computer Engineering, Kanazawa University, Ishikawa, Japan. His current research interests include photonic integrated devices on a silicon platform.

Dr. Maruyama is a member of the Japan Society of Applied Physics and the Institute of Electronics, Information, and Communication Engineers of Japan. He received the Hiroshi Ando Memorial Young Engineer Award from the Foundation of Ando Laboratory.



**Tadashi Okumura** (S’08–M’10) was born in Gifu prefecture, Japan, in 1983. He received the B.E., M.E., and Ph.D. degrees from the Tokyo Institute of Technology, Tokyo, Japan, in 2006, 2008, and 2010, respectively.

He joined the University of California, Santa Barbara, CA, in 2009 as a Visiting Scholar. His research interests include silicon photonics and membrane-based photonic devices for optical interconnection.

Dr. Okumura is a member of the Japan Society of Applied Physics. He received a Research Fellow for Young Scientists in the Japan Society for the Promotion of Science (JSPS), Japan.